Supplement of Earth Syst. Dynam. Discuss., 6, 1201–1235, 2015
http://www.earth-syst-dynam-discuss.net/6/1201/2015/
doi:10.5194/esdd-6-1201-2015-supplement

Earth System Dynamics
Discussions
Open Access

Supplement of

Are there multiple scaling regimes in Holocene temperature records?

T. Nilsen et al.

Correspondence to: T. Nilsen (tine.nilsen@uit.no)

1 Test of the Lomb-Scargle periodogram - random removal of data

The test presented in Sect. 3.2 of the main article is here expanded to include random removal of data. Systematically we remove 25%, 50% and 75% of the data points from Monte Carlo ensembles. Fig. 1 shows the estimated scaling exponent vs. the true exponent for the even sampling case, and when 25%, 50% and 75% of the data points are removed. The negative bias seen for β slightly higher than unity in the even sampling case in Fig. 1a is expected, and is present also in the standard periodogram. It is due to a spectral feature arising when the (continuous-time) fBm is sampled at discrete times; the spectrum flattens when the Nyquist frequency is approached for β slightly above unity, and leads to an underestimation of β if these frequencies are used in the fitting of a straight line in the log-log plot.

In Fig. 1b,c,d we observe that when more data is removed, β is gradually more underestimated. This can be explained from Fig. 2 which shows increasing power at the high frequencies when data is removed. The LSP method fits sinusoids to the data on different frequencies, and the low frequency variability is mostly unaffected by the removal of data. For the high frequencies on the other hand, removal of data allows good fit of sinusoids with larger amplitude.

Fig. 1 demonstrates that serious underestimation of β can result from applying the LSP to time series with randomly missing data, if the true β is larger than unity.

2 Additional wavelet power spectra figures

Fig. 3 shows the wavelet power spectra for the last glacial period of GRIP. We observe that the higher power on these time scales really corresponds to a scaling regime with $\beta > 1$.

Fig. 4 shows the Mexican hat and Morlet wavelet power spectra for the Holocene part of the EPICA ice core. From the Morlet power spectrum we observe that the power increases on time scales from 600 yr and longer in two main periods; around 3 kyr and 8 kyr BP.

Fig. 5 shows the wavelet power spectra for the last glacial period of EPICA. Also here the power is increased on millennial time scales over the entire period, i.e., the new scaling is not caused by specific time-localised events.

3 Analysis of additional four deep ice core time series

To support our results in the main article, we present here the analyses of additional four deep ice cores from Greenland and Antarctica. The Greenland ice cores are GISP2, (Grootes et al., 1993; Grootes and Stuiver, 1997) and NGRIP, (North Greenland Ice-Core project (NGRIP) members, 2004; Andersen et al., 2006; Vinther et al., 2006; Rasmussen et al., 2006; Svensson et al., 2008; Wolff et al., 2010). From Antarctica we include the Taylor dome ice core, (Steig et al., 2000), and Vostok, (Lorius et al., 1985; Jouzel et al., 1987, 1993).

For the Holocene and last glacial period, the time series are shown together with the results from the LSP analysis for each ice core. It has already been illustrated in the main article that the shape of the LSP is affected by the length of the time series from the last glacial period, so here we only provide one time series from last glacial period covering approximately 15 kyr - 90 kyr BP.

3.1 Results from the GISP2 and NGRIP ice cores

Figure 6 shows (a) the δ^{18}O time series of the Holocene part of the GISP2 ice core, and (b) the LSP for the same time series. No scale break is detected on centennial time scales, and the estimated $\beta \approx 0.2$. (c) shows the δ^{18}O time series of the Holocene part of the NGRIP ice core, and (d) the LSP for the same time series, where we estimate $\beta \approx 0.35$ and no scale break at centennial time scales.

Figure 7 displays (a) The δ^{18}O time series for the GISP2 ice core from the last glacial period, and (b) the LSP for the same time series, where we estimate $\beta \approx 1.1$. (c) shows the δ^{18}O time series

for the NGRIP ice core from the last glacial period, and (d) the LSP for the same time series with estimated $\beta \approx 1.4$.

3.2 Results from the Taylor and Vostok ice core

Figure 8 shows (a) the Holocene time series of the Taylor ice core, and (b) the LSP for the same time series where we estimate $\beta \approx 0.2$ for time scales shorter than 10^3 yr. (c) shows the Holocene time series from the Vostok ice core, and (d) the LSP for the same time series. Due to the poor temporal resolution of the Vostok paleotemperature time series, the LSP has few data points and the uncertanties are therefore larger for this time series than others studied. Further, the LSP is affected by the smoothing of the δD time series. This is observed as an abrupt decrease in power at the highest frequencies, and a linear fit should be avoided in this area. We obtain $\beta \approx 0.1$ from the LSP, but note that this time series can not be used to infer the scaling at centennial time scales.

Figure 9 shows (a) The δ^{18}O time series for the Taylor ice core from the last glacial period, and (b) the LSP for the same time period where we estimate $\beta \approx 1.9$. (c) shows the δD time series for the Vostok ice core from the last glacial period, and (d) the LSP for the same time period with estimated $\beta \approx 1.7$.

References

Andersen, K. K., Svensson, A., Johnsen, S. J., Rasmussen, S. O., Bigler, M., Röthlisberger, R., Ruth, U., Siggaard-Andersen, M.-L., Steffensen, J. P., Dahl-Jensen, D., Vinther, B. M., and Clausen, H. B.: The Greenland Ice Core Chronology 2005, 15-42 ka. Part 1: constructing the time scale, Quaternary Sci. Rev., 25, 3246–3257, Shackleton special issue 24, 2006.

Grootes, P. M. and Stuiver, M.: Oxygen 18/16 variability in Greenland snow and ice with 10^3 to 10^5-year time resolution, Journal of Geophysical Research: Oceans, 102, 26 455–26 470, doi:10.1029/97JC00880, 1997.

Grootes, P. M., Stuiver, M., White, J. W. C., Johnsen, S., and Jouzel, J.: Comparison of oxygen isotope records from the GISP2 and GRIP Greenland ice cores, Nature, 366, 552–554, doi:10.1038/366552a0, 1993.

Jouzel, J., Lorius, C., Petit, J. R., Genthon, C., Barkov, N. I., Kotlyakov, V. M., and Petrov, V. M.: Vostok ice core: a continuous isotope temperature record over the last climatic cycle (160,000 years), Nature, 329, 403–408, doi:10.1038/329403a0, 1987.

Jouzel, J., Barkov, N. I., Barnola, J. M., Bender, M., Chappellaz, J., Genthon, C., Kotlyakov, V. M., Lipenkov, V., Lorius, C., Petit, J. R., Raynaud, D., Raisbeck, G., Ritz, C., Sowers, T., Stievenard, M., Yiou, F., and Yiou, P.: Extending the Vostok ice-core record of palaeoclimate to the penultimate glacial period, Nature, 364, 407–412, doi:10.1038/364407a0, 1993.

Lorius, C., Jouzel, J., Ritz, C., Merlivat, L., Barkov, N. I., Korotkevich, Y. S., and Kotlyakov, V. M.: A 150,000-year climatic record from Antarctic ice, Nature, 316, 591–596, doi:10.1038/316591a0, 1985.

North Greenland Ice-Core project (NGRIP) members: High-resolution record of Northern Hemisphere climate extending into the last interglacial period, Nature, 431, 147–151, doi:10.1038/nature02805, 2004.

Rasmussen, S. O., Andersen, K. K., Svensson, A. M., Steffensen, J. P., Vinther, B. M., Clausen, H. B., Siggaard-Andersen, M.-L., Johnsen, S. J., Larsen, L. B., Dahl-Jensen, D., Bigler, M., Röthlisberger., R., Fischer, H., Goto-Azuma, K., Hansson, M. E., and Ruth, U.: A new Greenland ice core chronology for the last glacial termination, J. Geophys. Res-Atmos., 111, doi:10.1029/2005JD006079, 2006.

Steig, E. J., Morse, D. L., Waddington, E. D., Stuiver, M., Grootes, P. M., Mayewski, P. A., Twickler, M. S., and Whitlow, S. I.: Wisconsinan and Holocene Climate History from an Ice Core at Taylor Dome, Western Ross Embayment, Antarctica, Geogr. Ann. A., 82, 213–235, 2000.

Svensson, A., Andersen, K., Bigler, M., Clausen, H., Dahl-Jensen, D., Davies, S., Johnsen, S., Muscheler, R., Rasmussen, S., Röthlisberger, R., Seierstad, I., Steffensen, J., and Vinther, B.: A 60 000 year Greenland stratigraphic ice core chronology, Clim. Past, 4, 47–57, doi:10.5194/cp-4-47-2008, 2008.

Vinther, B. M., Clausen, H. B., Johnsen, S. J., Rasmussen, S. O., Andersen, K. K., Buchardt, S. L., Dahl-Jensen, D., Seierstad, I. K., Siggaard-Andersen, M.-L., Steffensen., J. P., Svensson, A., Olsen, J., and Heinemeier, J.: A synchronized dating of three Greenland ice cores throughout the Holocene, J. Geophys. Res-Atmos., 111, D13 102, doi:10.1029/2005JD006921, 2006.

Wolff, E. W., Chappellaz, J., Blunier, T., Rasmussen, S., and Svensson, A.: Millennial-scale variability during the last glacial: The ice core record, Quaternary Sci. Rev., 29, 2828–2838, doi:10.1016/j.quascirev.2009.10.013, 2010.

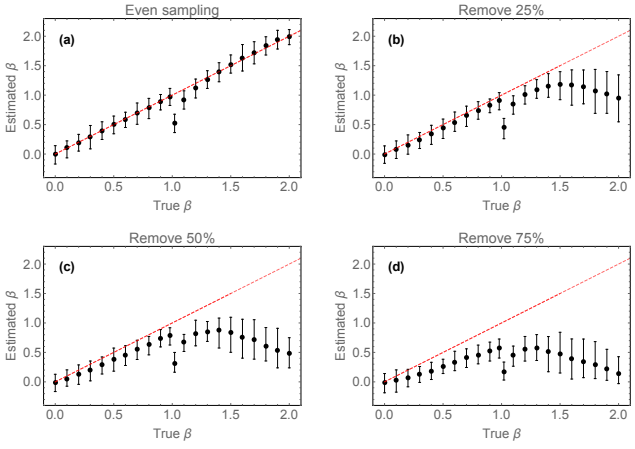

Figure 1. Value of estimated β vs. true β from 100 realizations of synthetic data. (a) Evenly sampled time series, 12576 data points. (b) 25% removed. (c) 50% removed. (d) 75% removed.

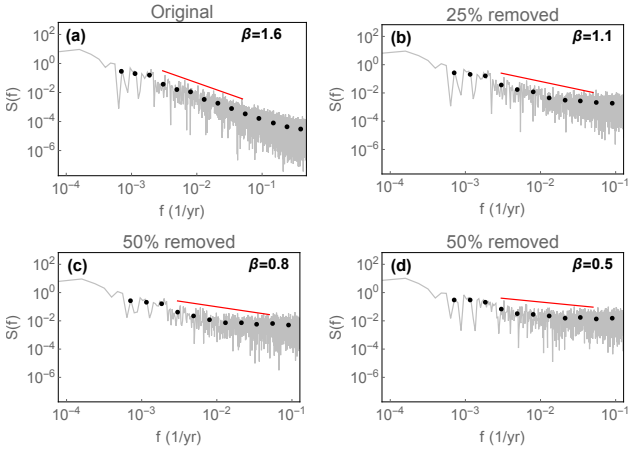

Figure 2. LSP for an fBm with β=1.6, with 12 576 data points. (a) Original time series. (b) 25% removed. (c) 50% removed. (d) 75% removed.

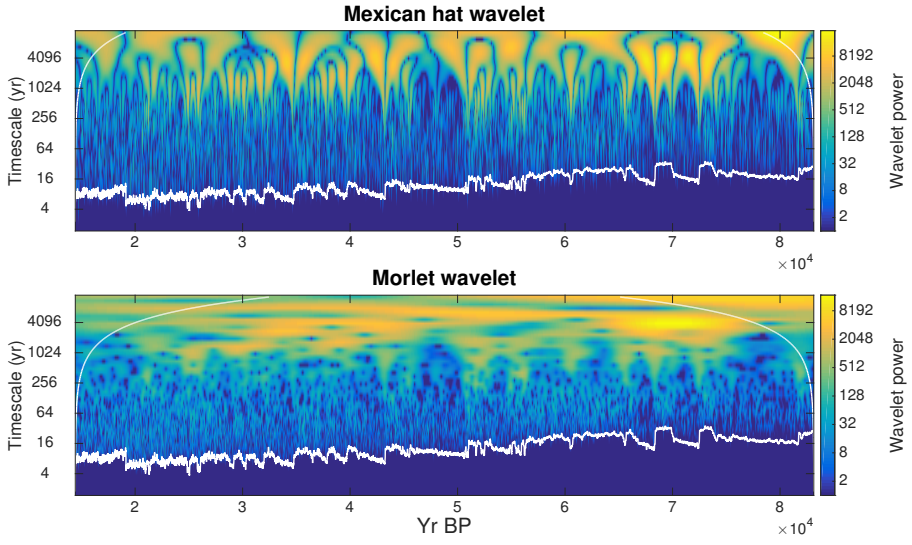

Figure 3. Top: the Mexican hat wavelet power spectrum for the last glacial part of the GRIP ice core, and bottom: the Morlet wavelet power spectrum for the same time series.

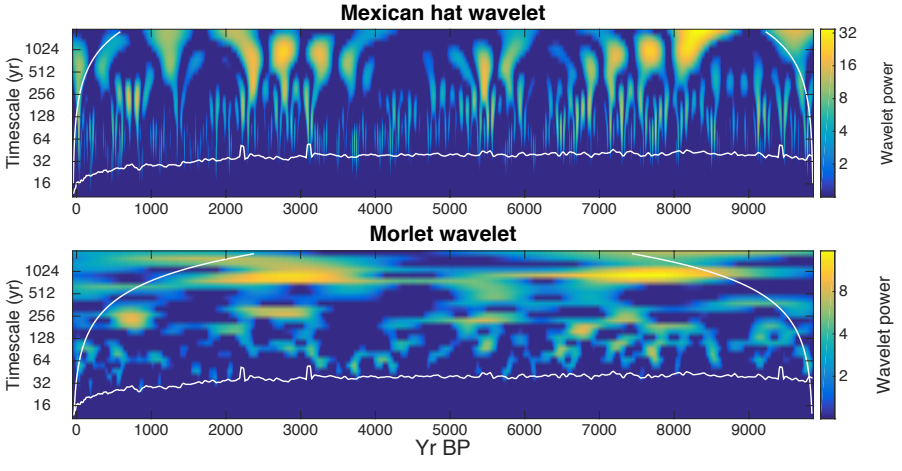

Figure 4. Top: the Mexican hat wavelet power spectrum for the Holocene part of the EPICA ice core, and bottom: the Morlet wavelet power spectrum for the same time series.

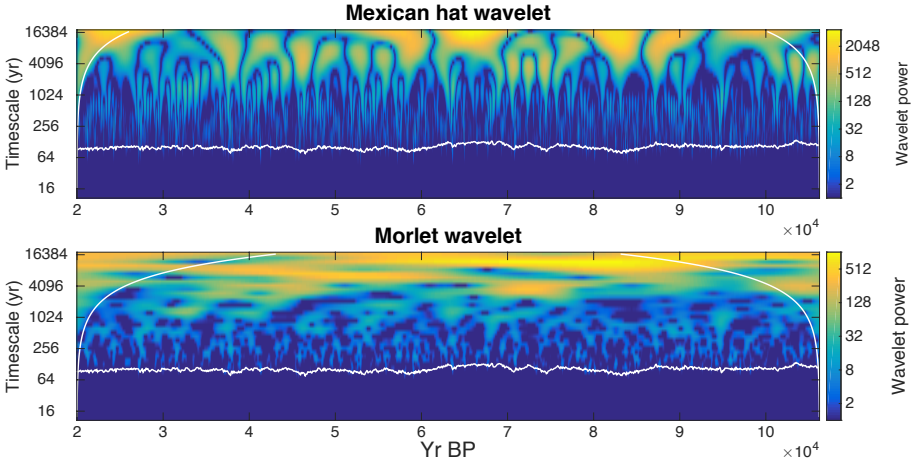

Figure 5. Top: the Mexican hat wavelet power spectrum for the last glaical part of the EPICA ice core, and bottom: the Morlet wavelet power spectrum for the same time series.

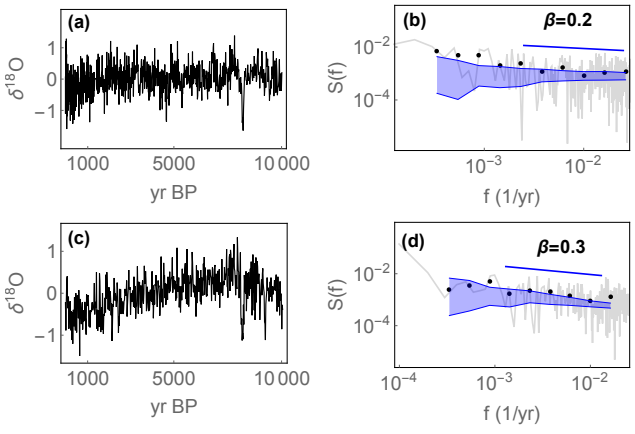

Figure 6. (a): δ^{18}O from the Holocene part of the GISP2 ice core. (b): Lomb-Scargle periodogram for the time series in (a). (c) δ^{18}O from the Holocene part of the NGRIP ice core. (d): Lomb-Scargle periodogram for the time series in (c). In (b) and (d) the raw LSP is shown in gray and the log-binned version by black dots. β is estimated from the log-binned LSP in the region marked by the blue line. The confidence range is shown by the shaded area, estimated from a Monte Carlo ensemble of synthetic fGn with the value of β found from the log-binned LSP.

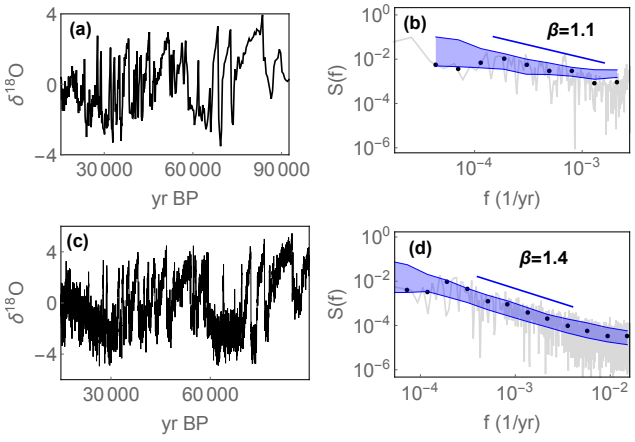

Figure 7. (a):^{18}O from the last glacial period part of the GISP2 ice core. (b): Lomb-Scargle periodogram for the time series in (a). (c): δ^{18}O time series from the last glacial period of the NGRIP ice core. (d): Lomb-Scargle periodogram for the time series in (c).

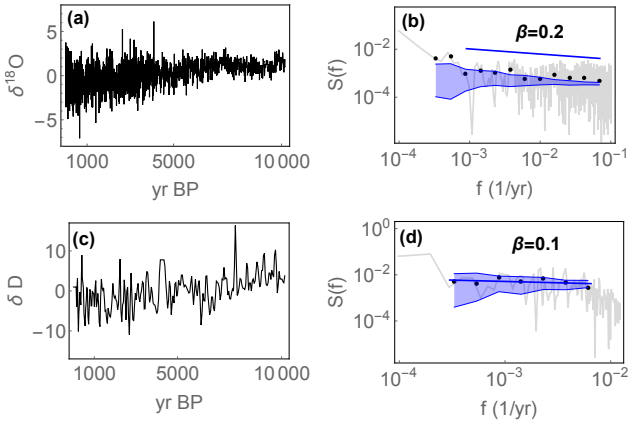

Figure 8. (a): δ^{18}O from the Holocene part of the Taylor ice core. (b): Lomb-Scargle periodogram for the time series in (a). (c) δD from the Holocene part of the Vostok ice core. (d): Lomb-Scargle periodogram for the time series in (c).

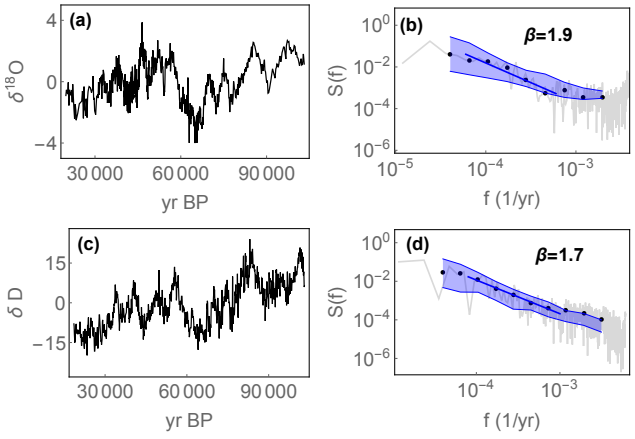

Figure 9. a): δ^{18}O from the last glacial period part of the Taylor ice core. (b): Lomb-Scargle periodogram for the time series in (a). (c):δD time series from the last glacial period of the Vostok ice core. (d): Lomb-Scargle periodogram for the time series in (c).